

APPENDIX; Parameters used in EHMO Calculation

Atom	s			p			d					
	n	-IP	ζ	n	-IP	ζ	n	-IP	ζ ₁	ζ ₂	c ₁	c ₂
H	1	13.6	1.30									
C(set 1)	2	21.4	1.625	2	11.4	1.625						
C(set 2)	2	21.4	1.92	2	12.67	1.92						
P	3	18.6	1.75	3	14.0	1.30						
Pd	5	7.32	2.19	5	3.75	2.152	4	12.02	5.983	2.613	0.5535	0.6701

Here, the Hückel constant, K is 1.75 and 2.35 in parameter set 1 and 2, respectively.

C₂H₄. In Pd-C₆₀ derivative type 1, two carbon sites of the double bond of C₆₀ localize electrons transferred from Pd-ligand.

Acknowledgment. This research was supported through KOSEF grant 94-080011013. We are grateful to Professor Y. Lee, KAIST, for his comment.

References

- Hawkins, J. M.; Meyer, A.; Lewis, T. A.; Stefan Loren; Hollander, F. J. *Science* **1991**, *252*, 312.
- Balch, A. L.; Catalano, V. J.; Lee, J. W. *Inorg. Chem.* **1991**, *30*, 3980.
- Fagan, P. J.; Calabrese, J. C.; Malone, B. *Science* **1991**, *252*, 1160.
- Fagan, P. J.; Calabrese, J. C.; Malone, B. *J. Am. Chem. Soc.* **1991**, *113*, 9408.
- Bashilov, V. V.; Petrovskii, P. V.; Sokolov, V. I.; Lindeman, S. V.; Guzey, I. A.; Struchkov, Y. T. *Organometallics* **1993**, *12*, 991.
- Amié, D.; Trinajstić, N. *J. Chem. Soc., Perkin Trans.* **1990**, *2*, 1595.
- Koga, N.; Morokuma, K. *Chem. Phys. Lett.* **1993**, *202*, 330.
- Fann, Y. C.; Singh, D.; Jansen, S. A. *J. Phys. Chem.* **1992**, *96*, 5817.
- Haddon, R. C.; Brus, E. L.; Raghavachari, K. *Chem. Phys. Lett.* **1986**, *125*, 459.
- Hale, P. D. *J. Am. Chem. Soc.* **1986**, *108*, 6087.
- Leach, S.; Vervloet, M.; Despres, A.; Breheret, E.; Hare, J. P.; Dennis, T. J.; Kroto, H. W.; Taylor, R.; Walton, D. R. M. *Chem. Phys.* **1992**, *160*, 451.
- (a) Hoffmann, R. *J. Chem. Phys.* **1963**, *39*, 1397. (b) Summerville, R. H.; Hoffmann, R. *J. Am. Chem. Soc.* **1976**, *97*, 7240. (c) Tatsumi, K.; Hoffmann, R.; Yamamoto, A.; Stille, J. K. *Bull. Chem. Soc. Jpn.* **1981**, *54*, 1857.
- Lee, K. H.; Lee, H. M. and Lee, W. R. *Bull. Kor. Chem. Soc.* **1995**, *16*, 226.

Electrical Properties of TiO_{2-x} Thin Films by Thermal Oxidation

Yong-Kook Choi*, Q-Won Choi†, Ki-Hyung Chjo, and Seung-Won Jeon

Department of Chemistry, Chonnam National University, Kwangju 500-757, Korea

†Department of Chemistry, Seoul National University, Seoul 151-742, Korea

Received February 23, 1995

The electrical properties of the TiO_{2-x} thin films prepared by thermal oxidation from titanium sheets have been studied. The films by water vapor oxidation are oxidized more homogeneously than those by air oxidation. The electrical contact to measure the electrical conductivity of the TiO_{2-x} electrodes is improved when the electrode surface is plated with silver. The hysteresis of the electrical conductivity curves is improved by applying alternating current rather than direct current on both sides of the electrode. The observed energy gap, E_d are 0.05-0.16 and 0.11-0.76 eV, respectively, at low and high temperatures region. These values of the TiO_{2-x} electrode prepared by water vapor oxidation are similar to those of single crystal TiO₂. The values of donor concentration, N_D , are observed about 10^{15} - 10^{19} and 10^{17} - 10^{21} cm⁻³, respectively, at low and high temperatures region. These values obtained at high temperature region are consistent with the values obtained from Mott-Schottky plot.

Introduction

The electrical and photo-electrochemical properties of

semiconductor electrodes have been studied for the purpose of changing the solar energy into an electrochemical energy.¹⁻³⁶ Many semiconductor materials have been used as

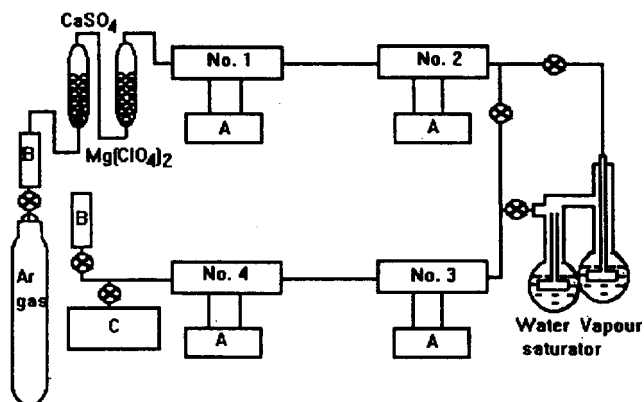


Figure 1. Apparatus for the preparation of TiO_{2-x} thin films and Ar-gas purification: No. 1) filled with Cu-turnings, No. 2) filled with Ti-turnings, No. 3) preheating furnace, No. 4) sample preparation furnace, A) temperature controller, B) rotameter, and C) apparatus for conductivity measurement.

photo-decomposition cells. Especially, TiO_2 and SrTiO_3 have been investigated by many researchers,²⁰⁻²⁵ because they are chemically stable in electrolyte solution. Electrical properties of single crystal TiO_2 have been also studied by Grant,³¹ Cronmeyer,³² Barbanel,³³ Breckenridge³⁴ and Hosler.³⁵ Cronmeyer³² also measured an electrical conductivity of reduced single crystal TiO_2 with the variation of temperature and reported that the electrical conductivity depends on temperature as an exponential function.

Breckenridge³⁴ and Hosler³⁵ also reported that the electrical conductivity of single crystal TiO_2 has two different energy levels at low and high temperatures region. In our previous studies,³⁰ we reported the photo-electrochemical properties of the TiO_{2-x} electrodes by thermal oxidation at low temperature and of the platinized TiO_2 electrodes. In the present study, we report the electrical properties of TiO_{2-x} thin films prepared by air and by water vapor oxidation at 600-1000 °C.

Experimental

TiO_2 thin films were prepared from titanium sheets ($1.0 \times 1.0 \times 0.10 \text{ cm}^3$, Nila Co., Japan, 99.999%), which were polished with alumina powder by using a Jasco Model DS-701G automatic crystal polisher (Japan). The titanium sheets were etched by dipping into a solution prepared by mixing 50 mL of HNO_3 , 30 mL of glacial acetic acid, 30 mL of HF, and a few drops of Br_2 . The etched sheets were rinsed with isopropyl alcohol, and dried in an oven at 50 °C for 1 hour. The titanium sheets were then used to form TiO_2 thin films by air oxidation in a Sybron Thermolyne-1300 furnace kept at 600, 700, 800, 900, and 1000 °C, respectively, for 1 min.

Figure 1 shows the apparatus used for the preparation of TiO_{2-x} thin films by water vapor oxidation. The titanium sheets were placed on the porcelain boat in No. 4 electric furnace, and temperatures of furnace were kept at 600, 700, 800, 900 °C, and 1000 °C, respectively. Cromel-Alumel thermocouples were used for the calibration of temperature in electric furnace. The TiO_{2-x} thin films were prepared by flowing Ar-gas saturated with the water vapor at 25 °C for

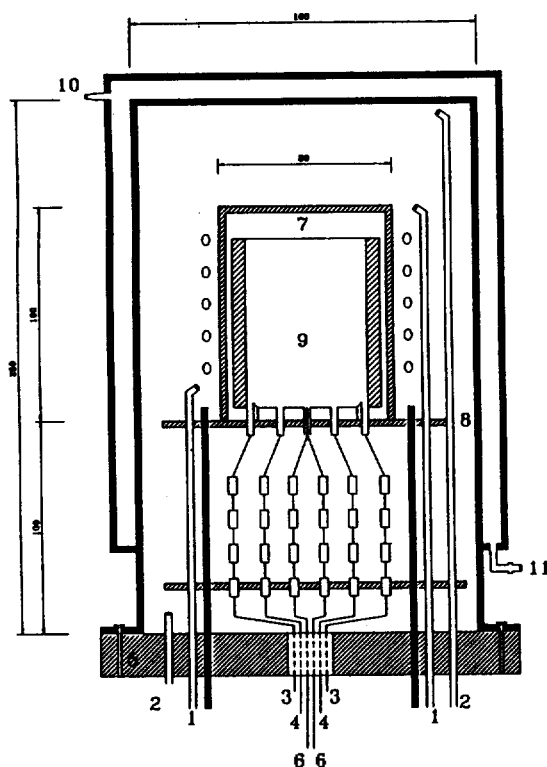


Figure 2. Triple wall chamber for measurement of electrical conductivity: 1) gas inlet, 2) gas outlet, 3) to voltage controller, 4) to circuit in Figure 4, 5) plank, 6) thermocouples, 7) stainless steel can, 8) stainless steel, 9) sample holder in Figure 3, 10) water inlet, 11) water outlet.

5 min (flow rate, 80 mL/min). The water vapor was the preheated at No. 3 furnace in Figure 1. Used Ar-gas (99.999%) in this study was purified by passing the CaSO_4 column, $\text{Mg}(\text{ClO}_4)_2$ column, stainless steel furnace (No. 1 in Figure 1) filled with Cu turnings kept at 300 °C, and stainless steel furnace filled with Ti turnings kept at 850 °C (No. 2 in Figure 1). The TiO_{2-x} thin films were then subjected to the atomic force microscopic (AFM, Park Scientific Instrument) analysis. The thicknesses of the films were calculated from the weight gain after the oxidation. Weight gains were measured by a L-SM semimicrobalance, with the precision of 10^{-6} g. Thicknesses of oxide films were then calculated by using a density of TiO_2 of 4.23 g/cm^3 with an assumption that the weight gain was solely due to the formation of the oxide film.

The TiO_{2-x} electrodes for the measurement of electrical conductivity were prepared by plating the TiO_{2-x} film surface with silver (area, 0.125 cm^2), and the other side was polished titanium metal. Electrical conductivity measurement was carried out with a home-building apparatus. Figure 2 and 3 show an apparatus for measuring the electrical conductivity of TiO_{2-x} electrodes with the variation of temperature. The oxygen in the chamber was eliminated by flowing purified Ar-gas for two hours at the flow rate of 80 mL/min. Home-building thermostat was used to control the temperature of the chamber. The electric heater in the chamber was covered with stainless steel case (the 7th part of Figure 2) in order to prevent the sample circumference from the thermal loss.

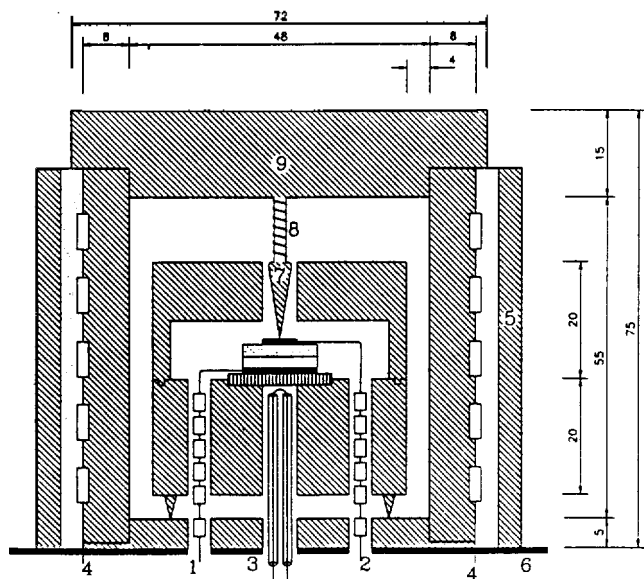


Figure 3. Sample holder for electrical conductivity measurement of TiO_{2-x} ; 1) to Ti metal, 2) to TiO_{2-x} film surface, 3) thermocouple, 4) heater, 5) asbestos, 6) stainless steel, 7) aluminum rod, 8) spring, 9) aluminum metal.

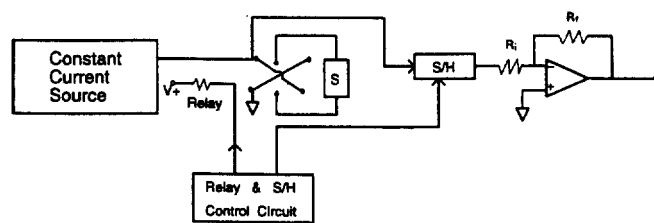


Figure 4. Block diagram of circuit for electrical conductivity measurement of TiO_{2-x} electrodes; S: sample(TiO_{2-x} electrode), S/H: sample-holder.

The water circulation device was used to control the temperature when temperature is lowered (see the 11th part of Figure 2). The electrical contact was improved by putting aluminum rod on the silver-plated TiO_{2-x} electrode.

Copper-Constantan thermocouples ($\phi = 1.4 \times 10^{-3}$ cm) were located under the Al_2O_3 plate to measure the temperature between titanium metal and TiO_{2-x} thin film. These temperature were recorded in the X-Y recorder by electromotive force unit after being corrected in the ice water (0°C). The electrical conductivity of the TiO_{2-x} electrode was measured by using the direct current (DC) or alternating current (AC) with the constant current source. The current direction was switched by using magnetic relay and sample-holder as shown in Figure 4. Capacitances were measured by Hewlett-Packard 4205B Universal Bridge at 1 KHz in order to obtain flatband potentials and donor densities of TiO_{2-x} films.

Result and Discussion

Average thicknesses of the TiO_{2-x} thin films prepared by air oxidation for 1 min and by water vapor oxidation for 5 min were calculated approximately 1990-2900 and 2000-

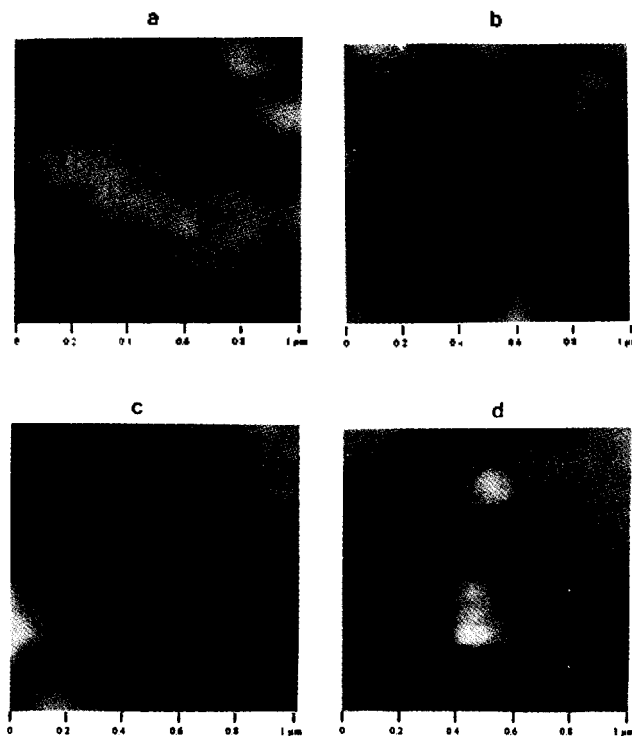


Figure 5. AFM pictures of a) 700 (VO), b) 800 (VO), c) 900 (VO), and d) 800 (AO), respectively. 700 (VO) and 800 (AO) indicate TiO_{2-x} thin film prepared by water vapor oxidation at 700°C and by air oxidation at 800°C .

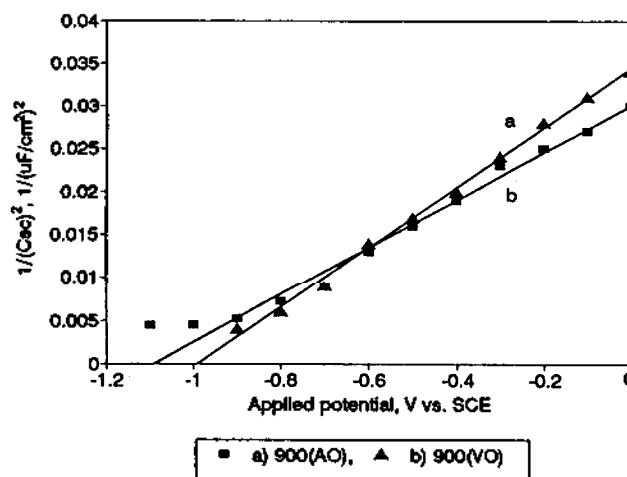


Figure 6. Mott-Schottky plots of a) a TiO_{2-x} electrode prepared by air oxidation of the Ti sheet at 900°C for 1 min. and b) TiO_{2-x} electrode prepared by water vapor oxidation of the Ti sheet at 900°C for 5 min.

3500 \AA , respectively (Table 1). The thicknesses of the TiO_{2-x} thin films were increased with the increase of furnace temperature. The thicknesses of TiO_{2-x} thin films by water vapor oxidation were thicker than those by air oxidation.

Figure 5 shows AFM pictures of TiO_{2-x} thin films. The surfaces of the films by water vapor oxidation at higher temperature were more homogeneous than those of lower tem-

Table 1. Flatband potentials and donor densities obtained from Mott-Schottky plot for TiO_{2-x} electrodes

Samples	Film thickness, Å	V _{fb} , vs. SCE	N _D , cm ⁻³
^a 600(AO)	1920	-0.96	9.2 × 10 ¹⁷
700(AO)	2140	-0.98	4.4 × 10 ¹⁸
800(AO)	2330	-0.98	7.1 × 10 ¹⁸
900(AO)	2570	-0.99	8.6 × 10 ¹⁸
1000(AO)	2900	-1.04	5.2 × 10 ¹⁹
^b 600(VO)	2010	-0.97	8.9 × 10 ¹⁸
700(VO)	2430	-0.97	3.7 × 10 ¹⁹
800(VO)	2720	-1.00	5.8 × 10 ¹⁹
900(VO)	3020	-1.10	6.2 × 10 ¹⁹
1000(VO)	3480	-1.10	6.9 × 10 ¹⁹
Single crystal		-1.08	6.5 × 10 ¹⁹

^aTiO_{2-x} electrode prepared by air oxidation of the Ti sheet at 600 °C, ^bTiO_{2-x} electrode prepared by water vapor oxidation of the Ti sheet at 600 °C.

perature counterparts. The surfaces of the films by air oxidation also partially were given island-like recrystallization. Although the AFM pictures cannot explain the molecular configuration state of the TiO_{2-x} film surface, the oxidized film surfaces can be compared with each other.

Flatband potentials and donor densities of TiO_{2-x} films were determined from intercepts and slopes of the Mott-Schottky plot²⁸

$$\frac{1}{C_x^2} = \frac{2}{\epsilon_0 \epsilon_x e N_D} \left(-\phi_x - \frac{kT}{e} \right) \quad (1)$$

where C_x is the capacitance, ε₀ and ε_x the electrical permittivity of vacuum and semiconductor, e the electrostatic charge, N_D the donor density, φ_x the potential drop in the space charge (V-V_{fb}), V the applied potential, V_{fb} the flatband potential, k the Boltzmann constant, and T the absolute temperature. Thus, the 1/C_x vs. electrode potential plot allows us to obtain flatband potential from intercept on the potential axis, which would be accurate to kT/e, and donor density from the slope. Figure 6 shows typical Mott-Schottky plots.

Table 1 lists flatband potentials and donor densities obtained from the Mott-Schottky analysis for TiO_{2-x} films. As shown in Table 1, the values of flatband potentials and donor densities were given -0.96-1.08 V and 10¹⁷-10¹⁹ cm⁻³, respectively. The results indicate that donor densities and flatband potentials are affected by the oxidation temperature of titanium sheets. Thus, the oxidation temperature appears to be important for the study on the properties of TiO_{2-x} films.

Various methods were tried to measure the electrical conductivity of the TiO_{2-x} electrodes. Figure 7 shows the resistance curve for the TiO_{2-x} electrode vs. to the temperature using the direct current. Figure 7(A) shows resistance curve measured when linking with silver-paste for electrical contact of copper wire on the TiO_{2-x} film surface, and Figure 7(B) shows resistance curve measured when silver-plating. Figure 7(a) and 7(b) also show resistance values measured while the temperature was lowered and raised, respectively. As

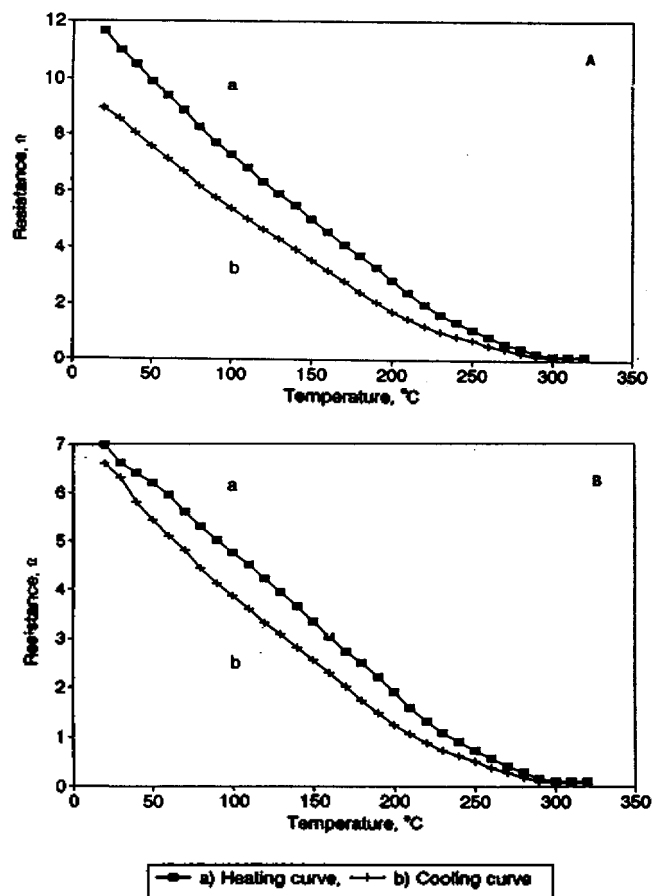


Figure 7. Electrical conductivity of 900 (VO) TiO_{2-x} electrode according to the temperature. The TiO_{2-x} surface was linked with silver-paste (A) and silver-plate (B).

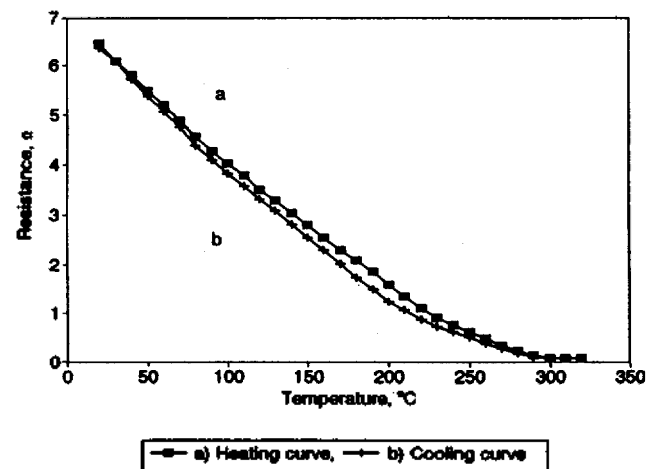


Figure 8. Electrical conductivity of 900 (VO) TiO_{2-x} electrode with AC according to the temperature. The TiO_{2-x} electrode surface was plated with silver.

shown in Figure 7, resistance gap between curve (a) and (b) is very small in case of the silver-plated TiO_{2-x} film. When silver-paste is used for electrical contact, resistance gap is slightly large because the ohmic contact of silver-paste

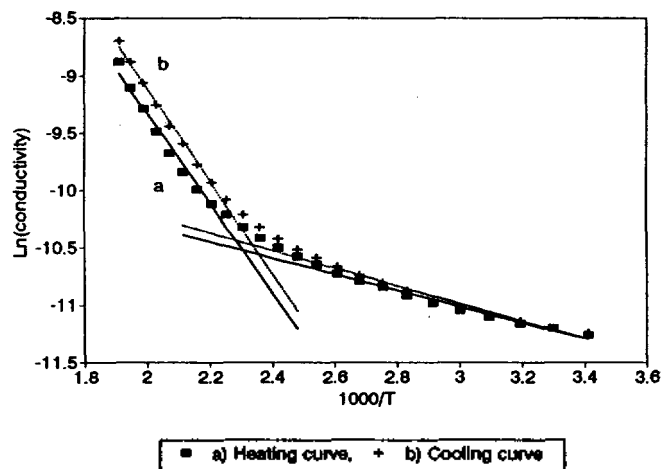


Figure 9. Plots of $\ln \sigma$ vs. $(1000/T)$ for same data shown in figure 8.

differs from the variation of temperature.

Figure 8 shows the resistance curve measured by changing the direction of current (AC) between Ti and TiO_{2-x} film. As shown in Figure 8, the value of resistance gap between (a) and (b) is more reduced than that measured by using DC. The energy gap ($E_C - E_D$, E_d) between the conduction band and donor level in the semiconductor is as follows.³⁶⁻³⁷

$$\sigma = \mu q (N_D N_C)^{1/2} / \sqrt{2} \exp[-(E_C - E_D) / 2kT] \quad (2)$$

In the Eq. (2) σ is electrical conductivity, N_C the effective density of states in the conduction band, E_C the energy at the bottom of the conduction band, E_D the energy of donor level, q the electronic charge, μ the mobility of the electron in TiO_{2-x} ($\approx 0.1 \text{ cm}^2/\text{V}$).³⁸ The energy gap can be obtained from the linear slope, when $\ln \sigma$ against $1/T$ is plotted. Breckenridge³⁴ reported that the electrical conductivity of reduced single crystal TiO₂ is given according to the two different lines. According to Breckenridge, Eq. (2) can be expressed as follows

$$\sigma = K_l e^{-E_d/2kT} + K_h e^{-E_{dh}/2kT} \quad (3)$$

In the Eq. (3), K is $\mu q (N_D N_C)^{1/2} / \sqrt{2}$ and E_d and E_{dh} are energy gap (E_d) at the low and the high temperature region, respectively. At the low temperature region, $E_d > E_{dh}$. Therefore, Eq. (3) is written as

$$\sigma_l = K_l e^{-E_d/2kT} \quad (4)$$

At the high temperature region, $E_d < E_{dh}$. There, the Eq. (3) is written as

$$\sigma_h = K_h e^{-E_{dh}/2kT} \quad (5)$$

According to Eq. (4) and Eq. (5), a plot of $\ln(\sigma)$ vs. $1000/T$ should yield a straight line with a slope of $E_d/2k$ and an intercept of $\ln K$.

The (a) and (b) in Figure 9 indicate the $\ln \sigma$ vs. $1000/T$ plots from the electrical conductivity measured while the temperature was raised or lowered. These plots show the straight lines with two different slopes and these results are the same for the TiO_{2-x} electrodes used in this study. The slope of low temperature ranges is due to excitation

Table 2. The values of film thickness and E_d for TiO_{2-x} electrodes

Samples	^a R		^b L	
	^c E_d , eV	^d E_{dh} , eV	^c E_d , eV	^d E_{dh} , eV
^a 600(AO)	0.051	0.11	0.052	0.12
700(AO)	0.066	0.23	0.064	0.24
800(AO)	0.092	0.59	0.094	0.61
900(AO)	0.140	0.62	0.150	0.63
1000(AO)	0.150	0.71	0.160	0.73
^a 600(VO)	0.100	0.51	0.110	0.50
700(VO)	0.130	0.60	0.130	0.62
800(VO)	0.150	0.72	0.160	0.74
900(VO)	0.160	0.73	0.170	0.75
1000(VO)	0.160	0.75	0.160	0.76

^aMeasurements were made while the temperature of TiO_{2-x} electrode was raised. ^bMeasurements were made while the temperature of TiO_{2-x} electrode was lowered. ^cThe value of $E_C - E_D$ at low temperature region. ^dThe value of $E_C - E_D$ at high temperature region. ^a600(AO): TiO_{2-x} electrode prepared by air oxidation of the Ti sheet at 600 °C. ^a600(VO): TiO_{2-x} electrode prepared by water vapor oxidation of the Ti sheet at 600 °C.

Table 3. The values of donor density for TiO_{2-x} electrodes

Samples	^a R		^b L	
	N_D , cm ⁻³	N_D , cm ⁻³	N_D , cm ⁻³	N_D , cm ⁻³
600(AO)	4.32×10^{15}	5.33×10^{17}	3.39×10^{15}	4.76×10^{17}
700(AO)	1.88×10^{16}	3.81×10^{18}	2.10×10^{16}	3.64×10^{18}
800(AO)	8.13×10^{17}	6.17×10^{19}	8.11×10^{17}	5.49×10^{19}
900(AO)	3.24×10^{18}	9.95×10^{19}	3.12×10^{18}	8.37×10^{19}
1000(AO)	7.29×10^{18}	3.59×10^{20}	6.98×10^{18}	3.44×10^{20}
600(VO)	2.92×10^{16}	1.77×10^{18}	2.84×10^{16}	1.68×10^{18}
700(VO)	4.95×10^{17}	2.65×10^{19}	3.77×10^{17}	2.63×10^{19}
800(VO)	6.12×10^{18}	8.19×10^{20}	6.02×10^{18}	8.02×10^{20}
900(VO)	1.22×10^{19}	1.24×10^{21}	1.21×10^{19}	1.16×10^{21}
1000(VO)	2.38×10^{19}	6.23×10^{21}	2.19×10^{19}	5.99×10^{21}

^aMeasurements were made while the temperature of TiO_{2-x} electrode was raised. ^bMeasurements were made while the temperature of TiO_{2-x} electrode was lowered.

of electron at the lowest conduction band from the first donor level. On the other hand, the slope of high temperature range is primarily a result of excitation of electrons to the lowest conduction band from the second donor level. The E_d value from the slope and the donor densities, N_D , from the intercept can be calculated in case that μ ($0.1 \text{ cm}^2/\text{V}$) and N_C ($2.51 \times 10^{19} \text{ cm}^{-3}$)³⁷ are known. The values of E_d and N_D are listed in Table 2 and Table 3. As shown in Table 2 and 3, E_d and N_D are almost the same whether the temperature is lowered or raised. We obtained E_d of 0.05-0.16 eV in the low temperature region (25-140 °C) and 0.11-0.76 eV in the high temperature region (150-320 °C). These values tend to increase for the TiO_{2-x} electrodes at high temperature. Breckenridge³⁴ observed a E_d of 0.1 eV in the low tem-

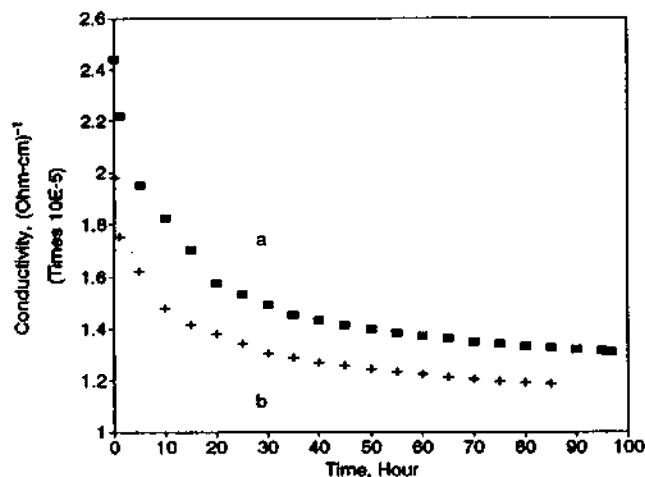


Figure 10. Variation of conductivity for 900 (VO) TiO_{2-x} electrode at constant temperature; a) at 50 °C and b) at 150 °C.

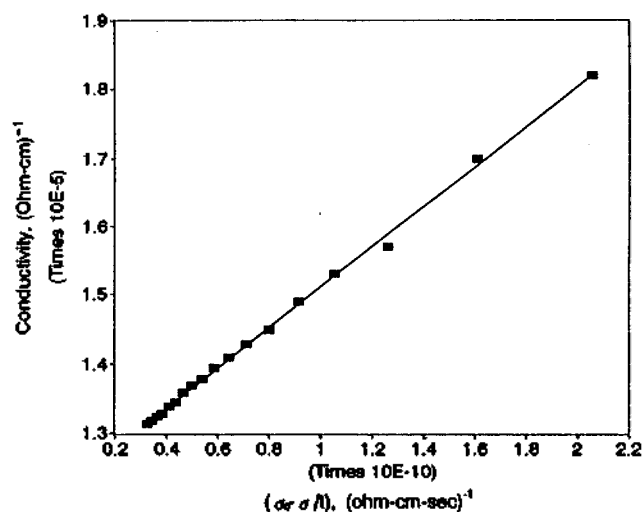


Figure 11. Plots of σ vs. $(\sigma_0 - \sigma)/t$ for data shown in Figure 10(a).

perature region and 0.2 eV in the high temperature from the electrical conductivity measurement of single crystal TiO_2 . We believe that ours and Breckenridge values are more consistent. In our study, the TiO_{2-x} thin films by air oxidation at 1000 °C have properties of single crystal TiO_2 . Otherwise, the TiO_{2-x} thin films by water vapor oxidation at 800-1000 °C have properties of single crystal TiO_2 . The values of N_D were $1015\text{-}1019\text{ cm}^{-3}$ in the low temperature region and $1017\text{-}1021\text{ cm}^{-3}$ in the high temperature. The values of N_D in the low temperature are similar to the value obtained from the Mott-Schottky plot. These values also agreed to that of Breckenridge's report³⁴ on the single crystal TiO_2 .

Figure 10 shows the electrical conductivity of the TiO_{2-x} electrode measured with the variation of to time at the constant temperature. The curve (a) and (b) indicate exponential function. Whitehurst⁴⁰ reported the equation of the electrical conductivity depending on time, as follows.

$$\sigma = \sigma_0 + B(\sigma_0 - \sigma)/t \quad (6)$$

Table 4. The values of B for 900(VO) TiO_{2-x} electrode at constant temperature

Temperature, °C	^a R	^b L
25	1.62×10^5	1.40×10^5
50	1.05×10^5	1.14×10^5
100	8.18×10^4	8.73×10^4
125	6.62×10^4	6.64×10^4
150	5.38×10^4	5.00×10^4
175	3.80×10^4	3.73×10^4
200	2.95×10^4	2.89×10^4
225	2.51×10^4	2.71×10^4
250	1.90×10^4	2.00×10^4

^aMeasurements were made while the temperature of TiO_{2-x} electrode was raised. ^bMeasurements were made while the temperature of TiO_{2-x} electrode was lowered.

In the Eq. (6), is the electrical conductivity at time t , σ_0 the electrical conductivity at $t=0$, σ_∞ the electrical conductivity maintained constantly equilibrium at $t=\infty$, B a factor at isothermal condition which is the reciprocal number of the rate constant. Figure 11 shows the plot σ against $(\sigma_0 - \sigma)/t$. The values of B were obtained from the slope, which was listed in Table 3. These values were comparatively corresponded with those which Whitehurst⁴⁰ measured for the single crystal TiO_2 and ceramic. In our study, the B values for the TiO_{2-x} electrodes by air oxidation at 1000 °C and by water vapor oxidation at the 800-1000 °C were corresponded with the electrical properties of the single crystal TiO_2 .

Conclusion

From the results of the electrical conductivity of the TiO_{2-x} thin film prepared by air oxidation and by water vapor oxidation, we conclude that:

1. The surfaces of TiO_{2-x} thin films prepared by water vapor oxidation are more homogeneous than those by air oxidation.
2. The electrical contact to measure the electrical conductivity of the TiO_{2-x} films is improved when the electrode surfaces are plated with silver on the TiO_{2-x} film.
3. The hysteresis of the electrical conductivity curves is improved by applying alternating current rather than direct current on both sides of the electrode.
4. The slopes of $\ln \sigma$ vs. $1000/T$ plots are given two branches. The E_d values are 0.05-0.16 eV in the low temperature region and 0.11-0.76 eV in the high temperature. Furthermore, the values of E_d of the TiO_{2-x} film by water vapor oxidation are consistent with the values that Breckenridge³⁴ indicated on the single crystal TiO_2 .
5. The values of donor densities are $10^{15}\text{-}10^{19}\text{ cm}^{-3}$ in the low temperature and $10^{17}\text{-}10^{21}\text{ cm}^{-3}$ in the high temperature. Donor densities are affected by the oxidation temperature of titanium metal sheet. These values are also consistent with the value obtained from Mott-Schottky plot.
6. The change of electrical conductivity of the TiO_{2-x} film with the variation of time at a constant temperature indicates the exponential function.

Acknowledgment. This work was supported by the

Basic Science Research Institute Program, Ministry of Education of Korea. Many thanks to professor Il-cheol Jeon, chonbuk university. He helped us with the AFM measurement of the sample.

References

1. Fujishima, A.; Honda, K. *Nature (London)* **1972**, *238*, 37.
2. Fujishima, A.; Kohayakawa, K.; Honda, K. *Bull. Chem. Soc. Jpn.* **1975**, *48*, 1041.
3. Fujishima, A.; Kohayakawa, K.; Honda, K. *J. Electrochem. Soc.* **1975**, *122*, 1487.
4. Laser, D.; Gottesfeld, S. *J. Electrochem. Soc.* **1978**, *125*, 358.
5. Hardee, K. L.; Bard, A. J. *J. Electrochem. Soc.* **1975**, *122*, 739.
6. Nozik, A. J. *Nature (London)* **1975**, *257*, 383.
7. Cooper, G.; Nozik, A. J. *J. Electrochem. Soc.* **1982**, *129*, 1973.
8. Wrighton, M. S.; Ellis, A. B.; Wolczanski, P. T.; Morse, D. L. *J. Am. Chem. Soc.* **1976**, *98*, 2774.
9. Mavroides, J. G.; Kafalas, J. A.; Kolesar, D. F. *Appl. Phys. Lett.* **1976**, *28*, 241.
10. Ellis, A. B.; Kaiser, S. W.; Wrighton, M. S. *J. Phys. Chem.* **1976**, *80*, 1325.
11. Kennedy, J. H.; Frese, K. W. *J. Electrochem. Soc.* **1976**, *123*, 1683.
12. Wrighton, M. S.; Morse, D. L.; Ellis, A. B.; Ginley, D. S.; Abrahamson, H. B. *J. Am. Chem. Soc.* **1976**, *98*, 44.
13. Williams, R. *J. Chem. Phys.* **1960**, *32*, 1505.
14. Ellis, A. B.; Kaiser, S. W.; Wrighton, M. S. *J. Am. Chem. Soc.* **1976**, *98*, 1635.
15. Anderson, W. W.; Chai, Y. G. *Energy Convers.* **1976**, *25*, 85.
16. Vanden Berghe, R. A. L.; Gomes, W. P. *Ber. Bunsenges. Phys. Chem.* **1972**, *76*, 481.
17. Yoneyama, H.; Sakamoto, H.; Tamura, H. *Electrochim. Acta.* **1975**, *20*, 341.
18. Nozik, A. J. *Appl. Phys. Lett.* **1976**, *29*, 150.
19. Candea, R. M.; Kastner, M.; Goodman, R. Hickok, N. *J. Appl. Phys.* **1976**, *47*, 2734.
20. Matsumoto, Y.; Shimizu T.; Sato, E. *Electrochim. Acta.* **1982**, *27*, 419.
21. Harting, K. J.; Getoff, H. *J. Hydrogen Energy* **1983**, *8*, 603.
22. Miller, D. *Chem. Phys. Lett.* **1983**, *100*, 236.
23. Morisaki, H.; Hariya, M.; Yazawa, K. *Appl. Phys. Lett.* **1977**, *30*, 7.
24. Decker, F.; Juliao, J. F.; Abramovich, M. *ibid.* **1979**, *35*, 397.
25. Kim, W. T.; Choe, C. H.; Choi, Q. W. *ibid.* **1981**, *39*, 61.
26. Chen, B. H.; White, J. M. *J. Phys. Chem.* **1982**, *86*, 3534.
27. Jaffrezic-Renault, N.; Pichat, P.; Foissy, A.; Mercier, R. *ibid.* **1986**, *90*, 2733.
28. Ghosh, A. K.; Maruska, H. P. *J. Electrochem. Soc.* **1977**, *124*, 1516.
29. Schottky, W. Z. *Phys.* **1942**, *118*, 539.
30. Choi, Y. K.; Seo, S. S.; Chjo, K. H.; Choi, Q. W.; Park, S. M. *J. Electrochem. Soc.* **1992**, *139*, 1803.
31. Grant, E. A. *Rev. Modern Physics* **1959**, *31*, 646.
32. Cronmeyer, D. C. *Phy. Review* **1952**, *87*, 876.
33. Barbanel, V. I.; Bogomolov, V. N.; Berodin, S. A.; Budarina, S. I. *Soviet Phy. Solid State* **1969**, *11*, 431.
34. Breckenridge, R. G.; Hosler, W. R. *Phy. Review* **1953**, *91*, 793.
35. Becker, J. H.; Hosler, W. R. *Phy. Review* **1965**, *137*, A1872.
36. Jarzebski, Z. M. *Oxide Semiconductor*; Pergaman Press: Oxford, 1973.
37. Sze, S. M. *Physics of Semiconductor Devices*; Wiley: New York, 1981; Chap. 1.
38. Subbarao, S. N.; Yun, Y. H.; Kershaw, R.; Dwight, K.; Wold, A. *Inorg. Chem.* **1979**, *18*, 488.
39. Mckelvey, J. *Solid State and Semiconductor Physics*; The Pennsylvania state university, 1969.
40. Whitehurst, H. B.; Morrison, J. J.; Endlish, F. L.; Warmkessel B. M.; Kevane, C. J. *J. Phys. Chem. Solids* **1967**, *28*, 861.